

2-Dimensional sheet structures from linked metal fluoride tetrahedra †

Lee A. Gerrard* and Mark T. Weller

Department of Chemistry, University of Southampton, Southampton, UK SO17 1BJ.
 E-mail: lag4@soton.ac.uk

Received 3rd July 2002, Accepted 27th September 2002
 First published as an Advance Article on the web 30th October 2002

Two 2-dimensional lithiumfluoroberyllate compounds, that possess identical anionic sheet topologies, have been synthesised from aqueous solutions under hydrothermal and ambient pressure conditions. The structures of $[\text{Li}_2\text{Be}_2\text{F}_8][\text{C}_2\text{N}_2\text{H}_{10}]$, **1**, and $[\text{Li}_2\text{Be}_2\text{F}_8][\text{CH}_3\text{NH}_3]_2\cdot[\text{H}_2\text{O}]_2$, **2**, consist of inorganic layers, constructed from linked $[\text{MF}_4]$ ($\text{M} = \text{Li}, \text{Be}$) tetrahedra with organic templating cations incorporated between the sheets. For the ethylenediammonium cation, **1**, the structure is a C -centred monoclinic cell, (space group $C2/c$), whereas the methylamine hydrate, **2**, crystallises in $P2_1/c$. The interlayer regions possess corrugated topologies within which the organic moieties lie with the amine groups directed into the larger pockets. Hydrogen bonding exists between ions situated on the protonated amine groups on the templating species and electronegative fluoride ions.

Introduction

Topologies constructed from vertex linked polyhedral units, such as tetrahedra and octahedra, are currently of considerable interest as a result of the properties of these frameworks which include porosity, ion exchange selectivity, and unusual electronic/magnetic behaviours derived from interacting metal ions at the polyhedra centres. Most such materials are based on oxide architectures,¹ as found with the oxo-tetrahedra building blocks of zeolites,² aluminosilicates, and aluminophosphates.³ Many other novel structures, with varying dimensionality including 1D chains,^{4,5} 2D sheets^{6–8} and 3D networks,⁹ have been synthesised using various organoamine templates.

Very few one, two and three-dimensional framework compounds are known that are constructed from $[\text{MF}_4]$ tetrahedral building units. Whereas Al^{3+} , Si^{4+} and P^{5+} are frequently used to counterbalance the oxide charge in zeolites and aluminophosphates, lower charged species such as M^{2+} and M^+ are required for fluoride ion analogues. For such compounds to maintain a tetrahedral geometry the metallic species is necessarily small, such as the first period elements Li, Be and B, thus avoiding a tendency for the cation co-ordination to expand to six. Only a few structures have been described that formally possess linked BeF_4 and LiF_4 tetrahedral units. One such class of materials which has frameworks built from linked tetrahedral fluoro-species is the bi-alkali metal beryllifluorides such as KLiBeF_4 adopting a tridymite type topology.¹⁰

The only other material based on linked MF_4 tetrahedra is lithium hydrazinium fluoroberyllate¹¹, $\text{Li}(\text{N}_2\text{H}_5)\text{BeF}_4$, which adopts the zeolite ABW structural topology. Formally this material can be considered in the same way as zeolites in that an organic templating agent, the hydrazinium cation, is present in pores formed from the linked fluoro-tetrahedra.

The idea of using templating agents, usually organo-amines, has produced a plethora of structural topologies both in phosphate-based and silicate-based networks but not, thus far, for fluorides. The most extensively used synthetic technique in the formation of these polyhedral framework structures is

reaction under hydrothermal conditions. Condensation of polyhedral units in the presence of a various templating species occurs rapidly under such conditions and has the advantage of leading to the growth of good quality crystals. The use of hydrothermal conditions as a route in synthesising zeolite,¹² aluminophosphate¹³ and other metallo-oxotetrahedral compounds,¹⁴ is thus widespread.

We describe here two fluoro-tetrahedral compounds that contain the same 2D-inorganic sheet topology but obtained with different templating agents. Compound **1**, $[\text{Li}_2\text{Be}_2\text{F}_8][\text{C}_2\text{N}_2\text{H}_{10}]$, was synthesised using ambient conditions with an organoamine that can be doubly protonated whereas compound **2**, $[\text{Li}_2\text{Be}_2\text{F}_8][\text{CH}_3\text{NH}_3]_2\cdot[\text{H}_2\text{O}]_2$, is prepared using a two-step hydrothermal and slow evaporation process with an amine that can be only singly protonated. Both materials contain terminal Be–F groups that might render them potentially useful in the synthesis of higher dimensionality materials through further condensation reactions.

Experimental

$[\text{Li}_2\text{Be}_2\text{F}_8][\text{C}_2\text{N}_2\text{H}_{10}]$ (**1**)

Ethylenediammonium orthofluoroberyllate (0.1 g, 67.97 mmol) was dissolved in distilled water (1 ml). Lithium carbonate (0.025 g, 33.98 mmol) was added to give an overall molar ratio of 2:1. The solution was placed in a polypropylene sample vial and left to slowly evaporate. The title compound crystallised to form colourless plate-like crystals. Finally, the product was recovered by filtration and air-dried. The yield for this reaction was very low therefore only allowing single crystal analysis.

$[\text{Li}_2\text{Be}_2\text{F}_8][\text{CH}_3\text{NH}_3]_2\cdot[\text{H}_2\text{O}]_2$ (**2**)

Beryllium fluoride (0.1 g, 0.002 mol) was dissolved in an acidic aqueous solution of distilled water (10 ml) and 30% hydrofluoric acid (0.17 ml, 0.004 mol). Methylamine 25–30% w/v solution in water (0.25 ml, 0.002 mol) was added and stirred. Finally lithium carbonate (0.07 g, 0.001 mol) was added to give an overall molar ratio of 2:4:2:1. The solution was placed in a 23 ml Teflon lined autoclave and heated at 80 °C for 24 h. After cooling the resulting solution was placed in a plastic sample vial

† Electronic supplementary information (ESI) available: rotatable 3-D structures of **1** and **2** in CHIME format. See <http://www.rsc.org/suppdata/dt/b2/b206469c/>

Table 1 Crystal data for **1** and **2**

	1	2
Molecular formula	CH ₅ NBeLiF ₄	CH ₈ NOBeLiF ₄
Crystal system	Monoclinic	Monoclinic
Space group	<i>C2/c</i>	<i>P2₁/c</i>
<i>a</i> /Å	19.467(4)	12.567(3)
<i>b</i> /Å	4.7968(10)	4.8493(10)
<i>c</i> /Å	9.867(2)	9.974(2)
β /°	106.98(3)	100.63(3)
<i>V</i> /Å ³	881.1(3)	597.4(2)
<i>Z</i>	8	4
μ /mm ⁻¹	0.224	0.188
Total no. of reflections	7349	3779
Independent reflections	1004	1047
<i>R</i> _{int}	0.0654	0.0564
<i>R</i> 1 [<i>I</i> > 2 σ (<i>I</i>)]	0.0370	0.0429
<i>wR</i> 2 [<i>I</i> > 2 σ (<i>I</i>)]	0.0913	0.0911

Table 2 Selected bond lengths (Å). Esds are given in parentheses

	1	2	
Li–F(1)	1.854(3)	Li–F(1)	1.860(4)
Li–F(1) ^a	1.875(3)	Li–F(1) ^c	1.878(4)
Li–F(2)	1.833(3)	Li–F(2)	1.836(4)
Li–F(3)	1.827(3)	Li–F(3)	1.828(4)
Be–F(1)	1.570(2)	Be–F(1) ^d	1.564(4)
Be–F(2) ^b	1.532(2)	Be–F(2)	1.527(4)
Be–F(3) ^a	1.558(2)	Be–F(3) ^e	1.550(3)
Be–F(4)	1.535(2)	Be–F(4)	1.543(3)

Symmetry transformations used to generate equivalent atoms:^a $-x+1/2, y-1/2, -z+1/2$. ^b $x, -y, z+1/2$. ^c $2-x+1, y+1/2, -z+1/2$. ^d $-x+1, -y, -z+1$. ^e $-x+1, -y+1, -z+1$.

Table 3 Selected bond angles (°). Esds are given in parentheses

	1	2	
F(1)–Li(1)–F(2)	108.09(13)	F(1)–Li(1)–F(2)	109.7(2)
F(1)–Li(1)–F(1) ^a	102.79(13)	F(1)–Li(1)–F(1) ^d	103.46(18)
F(1)–Li(1)–F(2) ^a	109.76(13)	F(1)–Li(1)–F(2) ^d	109.2(2)
F(1)–Li(1)–F(3)	106.60(13)	F(1)–Li(1)–F(3)	108.9(2)
F(2)–Li(1)–F(3)	120.82(14)	F(2)–Li(1)–F(3)	119.1(2)
F(3)–Li(1)–F(1) ^a	107.28(13)	F(3)–Li(1)–F(1) ^d	105.4(2)
F(1)–Be(1)–F(2) ^b	109.41(13)	F(1) ^e –Be(1)–F(2)	109.9(2)
F(1)–Be(1)–F(3) ^c	107.64(12)	F(1) ^e –Be(1)–F(3) ^f	108.5(2)
F(1)–Be(1)–F(4)	108.89(12)	F(1) ^e –Be(1)–F(4)	108.0(2)
F(3) ^c –Be(1)–F(4)	108.06(12)	F(3) ^f –Be(1)–F(4)	107.9(2)
F(2) ^b –Be(1)–F(3) ^c	107.92(12)	F(2)–Be(1)–F(3) ^f	108.8(2)
F(2) ^b –Be(1)–F(4)	114.69(13)	F(2)–Be(1)–F(4)	113.6(2)

Symmetry transformations used to generate equivalent atoms:
^{1a} $-x+1/2, y-1/2, -z+1/2$. ^b $-x+1/2, y-1/2, -z+1/2$. ^c $x, -y, z+1/2$.
^{2d} $-x+1, y+1/2, -z+1/2$. ^e $-x+1, -y, -z+1$. ^f $-x+1, -y+1, -z+1$.

and left to evaporate slowly. The title compound crystallised to form colourless plate-like crystals that were recovered by filtration and air-dried. Anal. calc. (%) for **2**: C, 8.46; H, 5.68; N, 9.86. Found: C, 8.10; H, 5.14; 9.66.

Characterisation

The crystal structures of **1** and **2** were determined from single-crystal X-ray diffraction data. Data were collected on a Nonius Kappa CCD Area detector diffractometer using Mo-K α radiation ($\lambda = 0.71073$ Å) ω and ϕ scans to fill the Ewald sphere at 120(2) K. The crystal structure parameters are described in Table 1. The structures were solved by direct methods using SHELXS-97¹⁵ and structure refinement by least-squares method SHELXL-97.¹⁵ All the calculations were performed using the WINGX¹⁶ system (Ver 1.64.03). All the non-hydrogen

atoms were refined anisotropically. Selected bond lengths and angles are listed in Tables 2 and 3.

CCDC reference numbers 189068 and 189069.

See <http://www.rsc.org/suppdata/dt/b2/b206469c/> for crystallographic data in CIF or other electronic format.

Results and discussion

The title compound, **1**, was formed using a pre-synthesised, co-crystallised organo-beryllium salt. The precursor, [BeF₄]-[C₂N₂H₁₀], was synthesised from an ambient reaction of beryllium fluoride, hydrofluoric acid and ethylenediamine that was left to slowly evaporate. The co-crystallisation of the templating agent, as a beryllium salt,¹⁷ aids the formation of these frameworks. The single crystal X-ray diffraction study performed on **1** shows that both the beryllium and lithium atoms lay at centres of slightly distorted fluorine tetrahedra. The Be–F bond lengths are between 1.535(2) and 1.570(2) Å and the F–Be–F angles range from 107.6(1)–114.7(1)°. These values are in good agreement with other [BeF₄]²⁻ geometries reported in the literature.^{17–19} The Li–F bond lengths occur over the range 1.827(3) to 1.875(3) Å with the F–Li–F angles distorted from tetrahedral, with values between 102.8(1) and 120.8(1)°. These are again in good agreement with other [LiF₄]²⁻ geometries described in the literature,¹⁹ Tables 2 and 3 and Fig. 1.

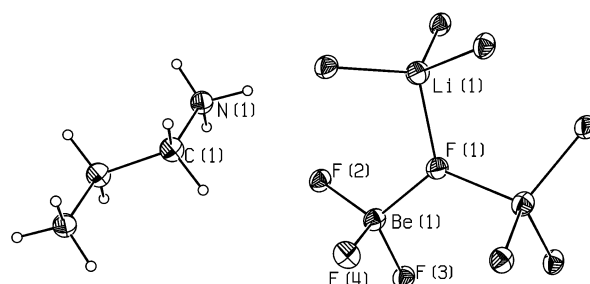


Fig. 1 The coordination geometry of the inorganic [Li₂Be₂F₈]²⁻ sheet and of the monomeric ethylenediammonium cation, clearly showing the μ_3 -fluoride, F(1). Ellipsoids shown are at the 30% probability level.

Each [BeF₄] unit vertex shares with four [LiF₄] tetrahedra through two doubly bridged and one triply bridged fluoride, F(1), leaving one terminal fluoride ligand. The terminal fluoride, F(4), is directed into the interlayer space to play a part in the N–H...F hydrogen bonding. The [LiF₄] moiety bonds to two [BeF₄] units through doubly bridged fluorides and links to two [BeF₄] and two other [LiF₄] units each through a triply shared vertex at F(1). The connectivity of the sheet, viewed down the *a* axis and formed from the linkages described above, produces a two-dimensional array that can be illustrated as an infinite sheet of *zz* chains forming ‘ladders’ of both T4 and T3 rings. The T4 rings alternate in a ‘double-diamond’ motif,²⁰ and are interspersed, above and below, with rows of triangular cavities, 3 nets, which point in opposing directions. Schematic and polyhedral arrangements for the anionic 2D sheet are shown in Fig. 2(a) and (b).

Consideration of a slice (viewed along the *bc* plane) through the three-dimensional network of tetrahedra in β -BeO,¹ shows a similar structural motif. The BeO topology has alternate 4 and 3 nets in two-dimensions whereas the compounds reported in this paper have rows of alternating nets, Fig. 2(b). Other similar fragments of the double-diamond topology have been observed in aluminophosphate sheets.²⁰

Perpendicular to the *a* axis the sheet can be viewed as a chain with [LiF₄] units coated either side by [BeF₄] tetrahedra. From the undulating nature of the sheet a ‘ladder’ motif is observed with nets in the form of a repeating unit of 4, 3, 3, 4... as shown in Fig. 3. The darker lines represent metal–metal linkages to aid the viewing. This diagram also clearly shows the

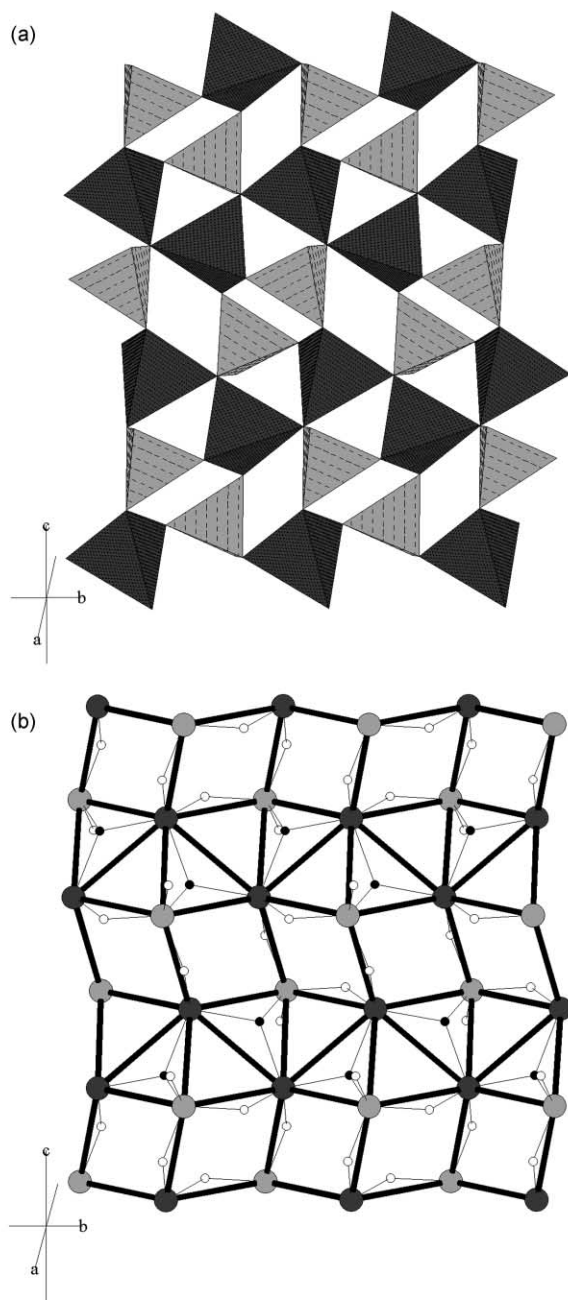


Fig. 2 (a) The polyhedral 2D sheet composed of $[\text{LiF}_4]$, dark hatching, and $[\text{BeF}_4]$, light hatching, tetrahedra, viewed along the a plane. (b) A schematic diagram showing the net topology through metal-metal linkages, Li – dark grey and Be – light grey. Small hollow spheres are terminal and doubly bridging fluoride and black spheres are the triply bridging fluoride atoms, F(1).

terminal fluorides that point into the channels to become involved in H-bonding.²¹

In the doubly protonated ethylenediammonium cation, distances of C–N 1.480(2) Å and C–C 1.510(3) Å are in good agreement with the average values reported previously for this group. The sheets pack in an AAAAA type formation running parallel to the a axis with an interlayer distance of $a/2$, 9.7335 Å. The organic moieties lie perpendicular to the inorganic sheets in ‘corrugated’ 2D channels. They align themselves at opposing maxima, formed by the undulating sheet, in the templated ‘pockets’. The doubly protonated organic cation sits in compartments which have a diameter ranging from 9.202–10.663 Å (Li \cdots Li), although the smallest channel width is of the order of 3.683–6.047 Å (F \cdots F).

The terminal $-\text{NH}_3$ groups hydrogen bond to the electro-negative fluorides on the rim of the 2D inorganic sheet. All

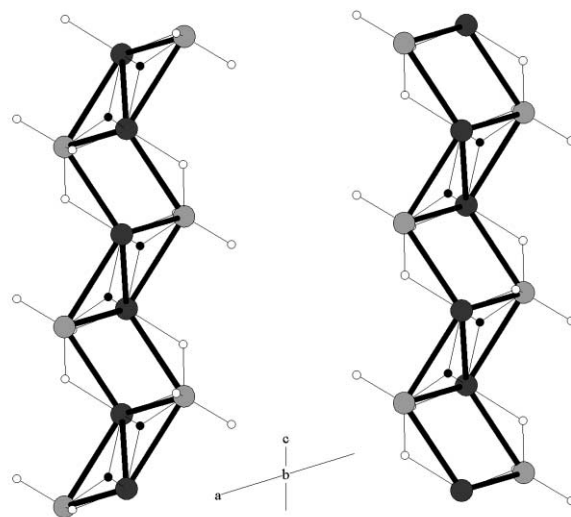


Fig. 3 The ‘ladder’ motif of two adjacent sheets, viewed down the b axis. The channel species inhabit the space between them. Li – dark grey and Be – light grey. Small hollow spheres are terminal and doubly bridging fluoride and black spheres are the triply bridging fluoride atoms, F(1).

three amino-hydrogen atoms are involved giving rise to six unique H-bonds, one trifurcated, one bifurcated and one singly bonded, that range from 2.7739(16) to 3.0183(16) Å.²¹ There are no H-bonded interactions to the triply bonded fluoride but the other three fluorides, two doubly and one terminal, each bifurcate two amino-hydrogen atoms. These link the layers together to form a three-dimensional hydrogen bonded network, Fig. 4. The hydrogen bond geometries are shown in Table 4.

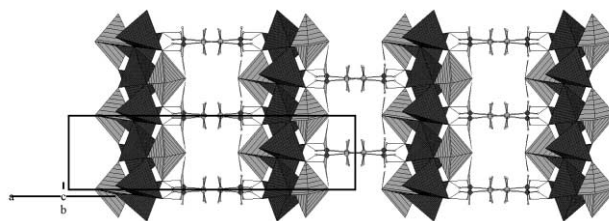


Fig. 4 Polyhedral view of the inorganic $[\text{Li}_2\text{Be}_2\text{F}_8]^{2-}$ sheets H-bonded to the ethylenediammonium cations. $[\text{LiF}_4]$ – dark hatching and $[\text{BeF}_4]$ – light hatching, light grey spheres – carbon, dark grey spheres – nitrogen, small hollow spheres hydrogen atoms and dashed lines H-bonds, viewed down the c axis.

The single crystal X-ray study undertaken on **2** shows the presence of the same lithioberyllofluoride layers as described for **1** with both beryllium and lithium lying at the centres of slightly distorted fluoride tetrahedra, Tables 2 and 3 and Fig. 5.

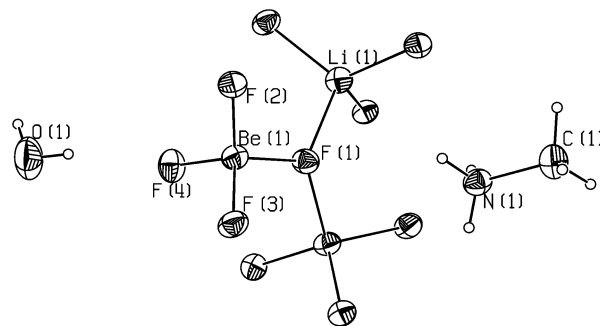


Fig. 5 ORTEP view of the three distinct moieties in the $[\text{LiBeF}_4]$ - $[\text{CH}_3\text{NH}_3][\text{H}_2\text{O}]$ complex. Ellipsoids shown at the 30% probability level.

Table 4 Hydrogen bonding geometry for **1** (Å, °)

D–H ⋯ A	<i>d</i> (D–H)	<i>d</i> (H ⋯ A)	<i>d</i> (D ⋯ A)	∠(DHA)
N(1)–H(1) ⋯ F(4) ^a	0.939(18)	2.116(18)	3.0183(16)	160.8(16)
N(1)–H(1) ⋯ F(3) ^b	0.939(18)	2.291(19)	2.9233(18)	124.2(14)
N(1)–H(2) ⋯ F(3) ^c	0.92(2)	2.04(2)	2.8530(17)	147.0(16)
N(1)–H(3) ⋯ F(4)	0.88(2)	1.90(2)	2.7739(16)	169(2)
N(1)–H(1) ⋯ F(2) ^a	0.94(2)	2.46(2)	2.805(2)	102(1)
N(1)–H(2) ⋯ F(2) ^a	0.91(2)	2.36(2)	2.805(2)	110(1)

Symmetry transformations used to generate equivalent atoms: **1**^a *x*, *y*+1, *z*. ^b $-x+1/2$, $y+1/2$, $-z+1/2$. ^c $-x+1/2$, $-y+1/2$, $-z$.

Table 5 Hydrogen bonding geometry for **2** (Å, °)

D–H ⋯ A	<i>d</i> (D–H)	<i>d</i> (H ⋯ A)	<i>d</i> (D ⋯ A)	∠(DHA)
N(1)–H(1) ⋯ F(4) ^a	0.85(4)	2.00(4)	2.831(3)	164(3)
N(1)–H(2) ⋯ F(4) ^b	0.88(3)	2.25(3)	3.099(3)	163(3)
N(1)–H(2) ⋯ F(3)	0.88(3)	2.32(3)	2.943(3)	128(2)
N(1)–H(3) ⋯ F(3) ^c	0.88(4)	2.10(4)	2.897(3)	149(3)
N(1)–H(3) ⋯ F(1) ^d	0.88(4)	2.75(3)	3.281(3)	120(2)
O(1)–H(7) ⋯ F(4) ^c	0.77(5)	1.95(5)	2.697(3)	164(5)
O(1)–H(8) ⋯ O(1) ^e	0.86(4)	1.84(4)	2.699(2)	176(4)

Symmetry transformations used to generate equivalent atoms: **2**^a $-x+1$, $-y$, $-z+1$. ^b $-x+1$, $-y+1$, $-z+1$. ^c *x*, $-y+1/2$, $z-1/2$. ^d $-x+1$, $y+1/2$, $-z+1/2$. ^e $-x+2$, $y+1/2$, $-z+1/2$.

Compound **2** has the same inorganic topology giving rise to the [Li₂Be₂F₈]²⁻ 2D sheet, lying parallel to the *bc* plane, as in Fig. 2. The sheets are at a much greater distance apart than in **1**, the separation being the length of the *a* axis at 12.567 Å, which gives rise to a greater volume for the interlayer molecules. Two different species reside in the channels, the templating organocations and solvent water molecules. The packing of the layers is in much the same style as **1**, with the 'pockets' accommodating two columns of methylammonium species and the narrowest region housing solvent waters.

In the interlayer region of compound **2**, the organo-template lies nearer the inorganic sheet with the solvent water molecules lying in a hydrogen bonded zigzag chain throughout the centre of the channel, zigzagging out of phase to the sheets, at a distance of 2.700(4) Å (O–H ⋯ O).²¹ The waters also interact weakly with the terminal fluorides, F(4), that point into the voids at a length of 2.697(3) Å (O–H ⋯ F), Table 5.

The methylamine NH₃ groups point toward the sheets leaving opposing CH₃ groups pointing diagonally into the same portion of the interlayer volume. The amino groups interact with the outermost fluorides giving rise to five unique H-bonds ranging from 2.004–2.394 Å (N–H ⋯ F).²¹ Again as observed in compound **1** the terminal fluorides have the most interactions with the amino hydrogen atoms whereas the triply bridging fluoride has no hydrogen bonding at all. The methylamine units alternate down either side of the channel, down the *b* axis, represented schematically in Fig. 6, although in reality they are situated above and below the plane of the schematic. A polyhedral representation, Fig. 7, shows all hydrogen bonding interactions through the three moieties. The methylamine cations are situated in similar positions as the ethylenediammonium species. The methyl groups form non-polar regions and therefore force the H-bonded chain of water molecules to lie at the centre of, furthest distance from, four columns of stacked methylammonium templates.

All N–H ⋯ F H-bonds, except one, have a separation that is shorter than the sum of the van der Waals radii of the hydrogen and fluorine. This suggests that there are indeed interactions between electronegative fluorine and the acidic hydrogen atoms from the protonated amines.

Caution: toxicity of beryllium is a chronic problem. Appropriate precautions should be taken whilst both handling and disposing of all beryllium-containing materials.

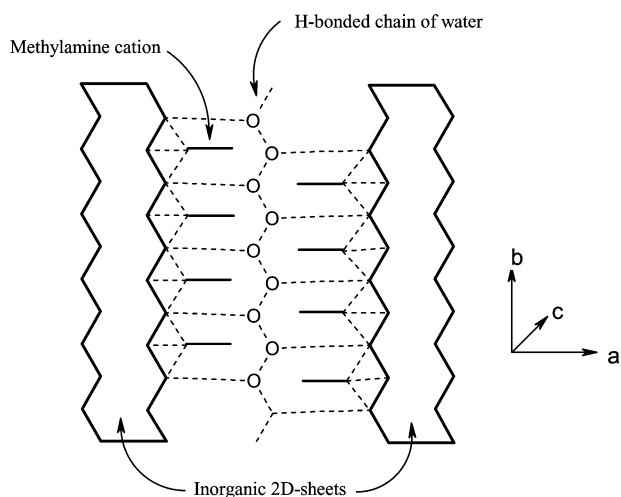


Fig. 6 Schematic diagram to show the snake-like H-bonded channels lying between two adjacent sheets (oxygen atoms shown), with the alternating organic cations, (thick black single lines) adding to the H-bonded 3D network. Dashed lines – H-bonds. Viewed along the *c* axis.

Conclusion

No two-dimensional sheet structures built from linked LiF₄ and BeF₄ tetrahedra templated with organoamines have been reported previously and hydrazinium lithiumorthofluoroberyllate¹¹ is the only Li/Be/F compound that has been synthesised using an organic cation in a role that could be considered as templating. This is in contrast to the extensive family of templated tetrahedral phosphate framework materials. Ethylenediamine,²⁰ methylamine⁹ and dabco (1,4-diazabicyclo[2.2.2]octane),²² have been used extensively to template many such structures. The use of tetrahedral [MF₄], where M = Li, Be, as a novel building block for 2 and 3 dimensional structures should thus be considered.

Acknowledgements

We wish to thank Prof. M. B. Hursthouse for access to the Kappa CCD diffractometer and the EPSRC for funding. Also Mr Alan Dickerson for the microanalysis result.

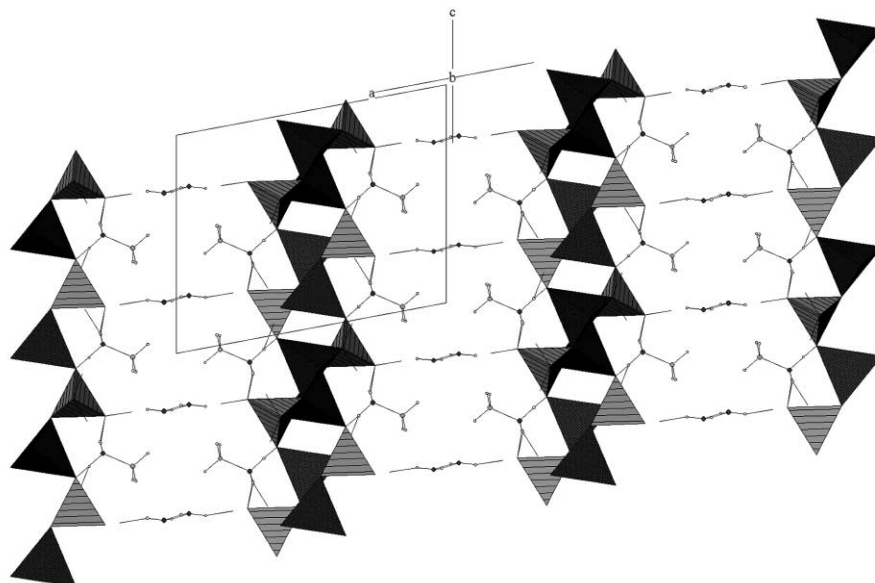


Fig. 7 Polyhedral representation of the H-bonded 3D network showing the interaction between the channel species and the 2D inorganic sheets. Same hatching scheme as Fig. 4.

References

- 1 A. F. Wells, *Philos. Trans. R. Soc. Lond., Ser. A*, 1986, **319**, 291–335.
- 2 R. M. Barrer, *Zeolites*, 1981, **1**, 130–140.
- 3 (a) R. E. Morris and S. J. Weigel, *Chem. Soc. Rev.*, 1997, **26**, 309–317; (b) J. M. Bennett, W. J. Dytrych, J. J. Pluth, J. W. Richardson and J. V. Smith, *Zeolites*, 1986, **6**, 349–361.
- 4 W. Chen, Y. S. Jiang, H. Huo, H. M. Yuan and J. S. Chen, *Chin. Chem. Lett.*, 2002, **13**, 474–477.
- 5 Q. Gao, J. Chen, S. Li, R. Xu, J. M. Thomas, M. Light and M. B. Hursthouse, *J. Solid State Chem.*, 1996, **127**, 145–150.
- 6 J. Yu, J. Li, K. Sugiyama, N. Togashi, O. Terasaki, K. Hiraga, B. Zhou, S. Qiu and R. Xu, *Chem. Mater.*, 1999, **11**, 1727–1732.
- 7 H. Yuan, G. Zhu, J. Chen, W. Chen, G. Yang and R. Xu, *J. Solid State Chem.*, 2000, **151**, 145–149.
- 8 I. D. Williams and J. Yu, *J. Solid State Chem.*, 1998, **136**, 141–144.
- 9 A. M. Chippindale, A. V. Powell, R. H. Jones, J. M. Thomas, A. K. Cheetham, Q. Huo and R. Xu, *Acta Crystallogr., Sect. C*, 1994, **50**, 1537–1540.
- 10 P. J. LeRoy and S. Aléonard, *Acta Crystallogr., Sect. B*, 1972, **28**, 1383–1387.
- 11 M. R. Anderson, I. D. Brown and S. Vilminot, *Acta Crystallogr., Sect. B*, 1973, **29**, 2625–2627.
- 12 (a) M. T. Weller and S. E. Dann, *Curr. Opin. Solid State Mater.*, 1998, **3**, 137–143; (b) G. A. Eimer, L. B. Pierella, G. A. Monti and O. A. Anunziata, *Catal. Lett.*, 2002, **78**, 65–75.
- 13 (a) A. Tuel, V. Gramlich and C. Baerlocher, *Microporous Mesoporous Mater.*, 2001, **46**, 57–66; (b) K. O. Kongshaug, H. Fjellvag and K. F. Lillerud, *Microporous Mesoporous Mater.*, 2000, **40**, 313–322.
- 14 (a) Y. N. Zhao, J. Ju, X. M. Chen, X. H. Li, R. J. Wang and Z. H. Mai, *J. Solid State Chem.*, 2002, **165**, 182–186; (b) Y. Xing, Y. L. Liu, Z. Shi, P. Zhang, Y. L. Fu, C. Cheng and W. Q. Pang, *J. Solid State Chem.*, 2002, **163**, 364–368.
- 15 Programs for Crystal Structure Analysis (Release 97-2). G. M. Sheldrick, Institut für Anorganische Chemie der Universität, Tammanstrasse 4, D-3400 Göttingen, Germany, 1998.
- 16 L. J. Farrugia, WINGX suite, *J. Appl. Crystallogr.*, 1999, **32**, 837–838.
- 17 B. Y. LeFur, S. Aléonard and M. F. Gorius, *Acta Crystallogr., Sect. C*, 1991, **47**, 949–951.
- 18 R. C. Srivastava, W. T. Klooster and T. F. Koetzle, *Acta Crystallogr., Sect. B*, 1999, **55**, 17–23.
- 19 J. C. Tedenac, S. Vilminot, L. Cot, A. Norbert and M. Maurin, *Mater. Res. Bull.*, 1971, **6**, 183–188.
- 20 (a) I. D. Williams, Q. Gao, J. Chen, L. Ngai, Z. Lin and R. Xu, *Chem. Commun.*, 1996, **15**, 1781–1782; (b) I. D. Williams, Q. Gao, J. Chen, J. Yu and R. Xu, *Chem. Commun.*, 1997, **14**, 1273–1274.
- 21 W. C. Hamilton and J. A. Ibers, *Hydrogen bonding in solids*, W. A. Benjamin, New York, 1968, 284.
- 22 S. Natarajan, S. Neeraj and C. N. R. Rao, *Solid State Sci.*, 2000, **1**, 87–98.